# Exploratory Synthesis with Molten Aluminum as a Solvent and Routes to Multinary Aluminum Silicides. $Sm_2Ni(Ni_xSi_{1-x})Al_4Si_6$ ($x = 0.18-0.27$): A New Silicide with a Ferromagnetic Transition at 17.5 K

X. Z. Chen,[†] S. Sportouch,[†] B. Sieve,[†] P. Brazis,[‡] C. R. Kannewurf,[‡] J. A. Cowen,[§] R. Patschke,[†] and M. G. Kanatzidis*[,†]

*Department of Chemistry and Center for Fundamental Materials Research, Michigan State University, East Lansing, Michigan 48824-1322, Department of Electrical and Computer Engineering, Northwestern University, Evanston, Illinois 60208-3118, and Department of Physics and Astronomy and Center for Fundamental Materials Research, Michigan State University, East Lansing, Michigan 48824-1322*

*Received April 17, 1998. Revised Manuscript Received June 23, 1998*

A new quaternary silicide, $Sm_2Ni(Ni_xSi_{1-x})Al_4Si_6$ ($x = 0.18-0.27$), has been synthesized from $Sm_2O_3$, NiO, and Si or Sm, Ni, and Si in Al metal flux at 800 °C. The structure, determined by single-crystal X-ray diffraction, is tetragonal, space group $P4/nmm$ (No. 129) with $Z = 2$, and lattice parameters $a = b = 5.8060(3)$ Å, $c = 14.845(1)$ Å. Refinement based upon $F^2$ [$I > 2\sigma(I)$] yielded $R1 = 0.0252$ and $wR2 = 0.0634$. The compound exhibits a new structure type containing two different alternating layers which are linked together through Si/Ni−Si bonds to form a three-dimensional framework. One layer is formed by edge-shared (the edges parallel to $c$) $NiAl_8$ cubes. The other layer is a Si-based net which consists of six-member, five-member, and square planar rings. The structure of this compound cannot be rationalized on the basis of the Zintl−Klemm concept. Extended Hückel, tight binding calculations were carried out for different hypothetical stoichiometries, besides the observed one, of the compound $Sm_2Ni(Ni_xSi_{1-x})Al_4Si_6$. Five models were investigated with $x = 0$, 0.25, 0.5, 0.75, and 1. The compounds with $x = 0$ and 0.25 are predicted to be more stable than the others. Electrical conductivity and thermopower data indicate that the compound is p-type metallic. The temperature-dependent magnetic susceptibility exhibits an antiferromagnetic ordering near 60 K and a weak ferromagnetic (WF) transition near 17 K. High temperature (150−300 K) magnetic susceptibility data suggest that Sm is in the 3+ oxidation state.

## Introduction

Silicides are both scientifically and technologically important and have been extensively studied during the past several decades. Because of their hardness, chemical stability, and high melting point silicides are well-known as high-temperature, oxygen-resistant structural materials[1] which are used, for example, in making high-temperature furnaces[2] and for high-temperature coatings.[3] Transition metal silicides are highly valued as electrical and magnetic materials, in addition to several new applications such as thermoelectric energy conversion[4] and compatible electrode materials in electronics.[5] It is also known that some silicides are low-temperature superconductors.[6] Several reviews and papers are available in the literature regarding their preparation, properties, crystal chemistry,[7] thermodynamics,[8] applications in silicon technology, [9] and materials aspects of silicides for advanced technologies.[10] Silicides are usually synthesized by direct reaction of the elements heated in a vacuum or in an inert atmosphere. The required reaction temperatures are usually over 1000

* To whom correspondence should be addressed: e-mail kanatzid@argus.cem.msu.edu.

[†] Department of Chemistry and Center for Fundamental Materials Research, Michigan State University.

[‡] Northwestern University.

[§] Department of Physics and Astronomy and Center for Fundamental Materials Research, Michigan State University.

(1) (a) Shah, D. M.; Berczik, D.; Anton, D. L.; Hecht, R. *Mat. Sci. Eng. A* **1992**, *155*, 45−57. (b) Meschter, P. J.; Schwartz, D. *J. Metals* **1989**, *41*, 52. (c) Inui, H.; Moriwaki, M.; Ito, K.; Yamaguchi, M. *Philos. Mag.* **1998**, *77*, 375.

(2) Fitzer, E. In *Plansee Proceedings 1955*; Benesovsky, F., Ed.; Pergamon: London, 1956; Chapter 7.

(3) Meier, G. H. In *High-Temperature Ordered Intermetallic Alloys II*; Stoloff, N. S., Koch, C., Liu, C. T., Izumi, O., Eds.; Materials Research Society Symposium Proceedings 81; Materials Research Society: Pittsburgh, 1987; p 443.

(4) CRC Thermoelectric Handbook and references therein.

(5) (a) Maex, K. *Mater. Sci. Eng. R−Rep.* **1993**, *11*, 53−153. (b) Murarka, S. P. *Silicides for VLSi Application*; Academic Press: New York, 1983; and references therein.

(6) King, R. B. *Inorg. Chem.* **1990**, *29*, 2164−2170 and references therein.

(7) Aronsson, B.; Lundström, T.; Rundqvist, S. *Borides, Silicides and Phosphides*; Methuen & Co. Ltd.: London, 1965.

(8) (a) Schlesinger, M. E. *Chem. Rev.* **1990**, *90*, 607−628. (b) Chart, T. G. *A Critical Assessment of Thermochemical Data for Transition Metal-Silicon Systems*; NPL report on Chemistry 18; National Physical Laboratory: Teddington, U.K., 1972.

(9) Reader, A. H.; Vanommen, A. H.; Weijs, P. J. W.; Wolters, R. A. M.; Oostra, D. J. *Rep. Prog. Phys.* **1993**, *56* (11), 1397−1467.

(10) Maex, K. *Appl. Surf. Sci.* **1991**, *53*, 328−337.

10.1021/cm980291z CCC: $15.00 © 1998 American Chemical Society
Published on Web 09/19/1998

°C, necessitating the use of an arc-welder or inductive furnace. Although single crystals sometimes can be obtained by annealing or quenching the product, only powder samples are obtained in most situations using these traditional methods. This often makes crystal structure determination more difficult and limits proper characterization. Some other less frequently used preparative methods for silicides are also known such as electrochemical synthesis[11] and chemical vapor-deposition.[12]

In this paper, we introduce a new synthetic approach for silicides—using molten Al as a solvent and metal oxide or pure metal element as precursors. We find that crystals of various aluminum silicides grow easily in Al melt below 1000 °C and so far we have discovered a large number of members of a new class of silicides. The oxide precursor method can be potentially extended to the synthesis of silicides by using silicates as precursors. Al fluxes have been used in the past to prepare borides[13] at very high temperature (>1400 °C). In the absence of Si or B, Al forms a variety of novel aluminides.[14] Because molten Al dissolves Si without forming a compound, we reasoned it may serve as a convenient solvent for delivery of Si atoms in a reaction. Therefore molten Al should serve as a useful medium for silicide synthesis particularly when it comes to preparing new compounds. In fact this approach works very well, as we have recently reported regarding the formation of the new family $Ln_2Al_3Si_2$ (Ln = Ho, Er, Tm) in Al flux.[15] Here we report the synthesis, structure, and magnetic and electrical properties of a new quaternary aluminum silicide $Sm_2Ni(Ni_xSi_{1-x})Al_4Si_6$ ($x = 0.18-0.27$) with a new structure type synthesized in Al flux.

## Experimental Section

**Synthesis.** Method 1—$Sm_2O_3$ (Rhone-Poulenc Inc. 99.99%), NiO (J. T. Baker Chemical Co.), Si (4N), and Al 20 mesh granular metal (Fisher, Co) were mixed in different molar ratios with excess of Al metal and the mixture was put into an alumina container which was flame sealed in a quartz tube under high vacuum. The sample was then heated to 800 °C, kept at that temperature for 8 days, and finally cooled to 300 °C (−5.2 deg/h). Method 2—In a $N_2$-filled drybox, Sm, Ni, Si, and Al were mixed in different molar ratios with excess of Al metal and transferred into an alumina tube which was sealed in a quartz tube as described above. The sample was first heated at 1000 °C for 15 h, then cooled to 860 °C in 10 h, kept at 860 °C for 4 days, and finally cooled to 360 °C (−10.4 deg/h). In both methods, NaOH(aq) solution was used to remove excess Al flux in the product. The single crystals used for electrical conductivity and magnetic susceptibility measurements were selected from the product made from method 2.

**EDS Analysis.** Semiquantitative microprobe analysis of the compound was performed with a JEOL JSM-35C scanning electron microscope (SEM) equipped with a Tracor Northern energy dispersive spectroscopy (EDS) detector. Data were acquired by using an accelerating voltage of 20 kV and 100-s accumulation time. A total of 46 crystals, obtained from the two different synthetic methods with different starting molar ratios of Sm:Ni, were examined with EDS. The results were quite consistent with an average formula of $Sm_{2.0}NiAl_{3.5}Si_{3.7}$. It was found that the composition of Al and Si from EDS is always lower than that obtained from X-ray refinement and, in this particular case, the correction factors of 1.14 for Al and 1.82 for Si should be applied to the results.

**Table 1. Crystallographic Data for $Sm_2Ni(Ni_xSi_{1-x})Al_4Si_6$ ($x = 0.27$)**

| | |
|---|---|
| formula weight | 672.23 |
| crystal system | tetragonal |
| space group | $P4/nmm$ (No. 129) |
| crystal size | 0.13 × 0.07 × 0.13 mm |
| $a$ | 5.8060(3) Å |
| $b$ | 5.8060(3) Å |
| $c$ | 14.845(1) Å |
| $V$ | 500.43(5) Å$^3$ |
| $Z$ | 2 |
| $d_{calc}$ | 4.449 g cm$^{-3}$ |
| $\theta$ range | 2.74−28.42° |
| diffractometer | Siemens smart platform CCD |
| index ranges | $-7 \le h \le 5$, $-7 \le k \le 7$, $-19 \le l \le 16$ |
| exposure time (s) | 15 |
| reflections collected | 3070 |
| temp (°C) | 25 |
| unique reflections | 419 [$R$(int) = 0.0407] |
| Radiation | Mo Kα ($\lambda = 0.71073$ Å) |
| $\mu$ | 14.928 mm$^{-1}$ |
| goodness of Fit | 1.101 |
| $R$ indices [I>2$\sigma$(I)][a] | $R1 = 0.0252$, $wR2 = 0.0634$ |
| $R$ indices (all data) | $R1 = 0.0324$, $wR2 = 0.0663$ |
| max peak and hole in final diff. electron density map | 1.554 and −2.038 e/Å$^3$ |

[a] $R1 = \Sigma||F_o| - |F_c||/\Sigma|F_o|$ and $wR2 = [\Sigma(|F_o^2 - F_c^2|)^2/\Sigma(wF_o^2)^2]^{1/2}$.

**X-ray Crystallography.** Single-crystal X-ray diffraction data were first collected on a crystal from synthetic method 1 using a Siemens SMART CCD diffractometer with Mo Kα ($\lambda = 0.71073$ Å) radiation. Absorption correction was applied to the data (SADABS; Sheldrick 1996); cell refinement and data processing were then performed with the program SAINT.[16] The structure was solved by direct methods (SHELXS86[17]) with the TEXSAN[18] crystallographic software package. The structure was refined with the SHELXL[19] package of programs. After the crystal structure was solved, to check the consistency of the stoichiometry with respect to the Ni/Si ratio in the formula, structural refinements were also performed on three other crystals, which were selected from the product of synthetic method 2 using two different molar ratios of starting materials. The crystallographic and refinement data are listed in Tables 1 and 2. All four crystals gave almost the same atomic positions, temperature factors, and bond distances and angles. The atomic positions and bond distances and angles are listed in Tables 3 and 4, respectively.

The large $U$ values of Si(4) and Ni(1)/Si(1) have been particularly scrutinized and the refinements of occupancies of the two sites did not show the presence of nonstoichiometry. Different possible structural models with the orthorhombic space group were also tried but the temperature factors became worse. The presence of a possible superlattice was also considered. The CCD data also suggested a supercell with $a = 8.2061(3)$ Å, $b = 8.2152(3)$ Å, and $c = 14.8447(2)$ Å but

(11) Shapoval, V. I.; Malyshev, V. V.; Novoselova, I. A.; Kushkhov, K. B. *Russ. J. Appl. Chem.* **1994**, *67*, 828−833.
(12) Madar, R.; Thomas, N.; Bernard, C. *Mater. Sci. Eng. B* **1993**, *17*, 118−125 and references therein.
(13) Okada, S.; Yu, Y.; Lundström, T.; Kudou, K.; Tanaka T. *Jpn. J. Appl. Phys.* **1996**, *35*, 4718−4723.
(14) (a) Nieman, S.; Jeitschko, W. *J. Solid State Chem.* **1995**, *114*, 337−341. (b) Nieman, S.; Jeitschko, W. *Z. Kristallogr.* **1995**, *210*, 338−341. (c) Nieman, S.; Jeitschko, W. *J. Solid State Chem.* **1995**, *116*, 131−135. (d) Nieman, S.; Jeitschko, W. *J. Alloys Comp.* **1995**, *221*, 235−239.
(15) Chen, X. Z.; Brazis, P.; Kannewurf, C. R.; Cowen, J. A.; Crosby, R.; Kanatzidis, M. G., submitted.
(16) SAINT, version 4; Siemens Analytical X-ray Instruments Inc., Madison, WI.
(17) Sheldrick, G. M. In *Crystallographic Computing 3*; Sheldrick, G. M., Kruger, C. C., Doddard, R., Eds.; Oxford University Press: Oxford, U.K., 1985; pp 175−189.
(18) "TEXSAN"—TEXRAY Structure Analysis Package; Molecular Structure Corporation: The Woodlands, TX, 1992.
(19) Sheldrick, G. M. 1995, SHELXL. Structure Determination Programs, Version 5.0. Siemens Analytical X-ray Instruments Inc., Madison, WI.

**Table 2. Crystallographic Data for Three Different Crystals of $Sm_2Ni(Ni_xSi_{1-x})Al_4Si_6$**

| | | | |
|---|---|---|---|
| refined $x$ value | 0.18 | 0.19 | 0.23 |
| formula weight | 669.57 | 669.88 | 671.10 |
| reaction condition | $Sm_2O_3$ + NiO + Al + Si | Sm + Ni + Al + Si | Sm + Ni + Al + Si |
| starting molar ratio | 1:1:40:5 | 4:1:12:8 | 2:1:12:7 |
| reaction temp (°C) | 800 | 860 | 860 |
| EDS analysis | $Sm_2NiAl_{2.2}Si_{3.4}$ | $Sm_{2.2}NiAl_{3.6}Si_{3.8}$ | $SmNiAl_{2.3}Si_{1.9}$ |
| crystal size (mm) | 0.18 × 0.21 × 0.03 | 0.13 × 0.13 × 0.04 | 0.09 × 0.09 × 0.04 |
| $a$ (Å) | 5.8161(2) | 5.8214(1) | 5.8191(1) |
| $b$ (Å) | 5.8161(2) | 5.8214(1) | 5.8191(1) |
| $c$ (Å) | 14.8603(3) | 14.8772(3) | 14.9010(0) |
| $V$ (Å$^3$) | 502.68(2) | 504.17(2) | 504.59(1) |
| data collect temp | 25 °C | −100 °C | 25 °C |
| $d_{calc}$ (g cm$^{-3}$) | 4.423 | 4.412 | 4.416 |
| $\theta$ range (deg) | 1.37−27.09 | 2.74−28.29 | 2.73−28.35 |
| index ranges | $-7 \le h \le 5$ | $-4 \le h \le 7$ | $-7 \le h \le 6$ |
| | $-6 \le k \le 7$ | $-7 \le k \le 6$ | $-7 \le k \le 5$ |
| | $-18 \le l \le 13$ | $-18 \le l \le 19$ | $-17 \le l \le 19$ |
| exposure time (s) | 30 | 20 | 15 |
| reflections collected | 2730 | 3125 | 3083 |
| unique reflections | 371 | 416 | 416 |
| $R$(int) | 0.047 | 0.032 | 0.0367 |
| $\mu$ (mm$^{-1}$) | 14.818 | 14.783 | 14.803 |
| goodness of fit | 1.719 | 1.275 | 1.108 |
| $R1$/w$R2$ [I>2$\sigma$(I)][a] | 0.0432/0.101 | 0.024/0.0706 | 0.0247/0.0624 |
| $R1$/$wR2$ (all data) | 0.0461/0.102 | 0.0289/0.0723 | 0.0305/0.0646 |
| residue peak (e/Å$^3$) | 2.127/−2.831 | 1.101/−1.109 | 1.391/−2.242 |

[a] $R1 = \Sigma||F_o| - |F_c||/\Sigma|F_o|$ and $wR2 = [\Sigma(|F_o^2 - F_c^2|)^2/\Sigma(wF_o^2)^2]^{1/2}$.

**Table 3. Atomic Positions and Equivalent Isotropic Displacement Parameters (Å$^2$) for $Sm_2Ni(Ni_xSi_{1-x})Al_4Si_6$ ($x = 0.27$)**

| | position | $x$ | $y$ | $z$ | $U$(eq)[a] | occ |
|---|---|---|---|---|---|---|
| Sm | 4f | 0.75 | 0.25 | 0.2643(1) | 7(1) | 1 |
| Ni | 2a | 0.75 | 0.25 | 0 | 6(1) | 1 |
| Al | 8j | 0.4959(2) | 0.0041(2) | 0.0891(1) | 7(1) | 1 |
| Si(1) | 2c | 0.75 | 0.75 | 0.3587(2) | 20(1) | 0.73(1) |
| Ni(1) | 2c | 0.75 | 0.75 | 0.3587(2) | 20(1) | 0.27(1) |
| Si(2) | 2c | 0.75 | 0.75 | 0.1964(2) | 6(1) | 1 |
| Si(3) | 2c | 0.25 | 0.25 | 0.2059(2) | 8(1) | 1 |
| Si(4) | 8j | 0.4611(3) | 0.0389(3) | 0.4218(1) | 23(1) | 1 |

[a] $U$(eq) is defined as one-third of the trace of the orthogonalized $U_{ij}$ tensor.

was likely caused by the problem of $\lambda/2$ radiation. SHELXL[19] tended to transform the supercell back to our original cell. After carefully examining the data with this "supercell", the only reasonable cell is C-centered orthorhombic. *Cmma* (No. 67) was the only possible centrosymmetric space group based on the systematic absence conditions. The refinement was unstable, the $R1$ factor could not be improved below 12%, and the temperature factors for one Si atom were unreasonably large. Electron diffraction studies, which are sensitive to the presence of long-range modulations, confirmed the tetragonal cell parameters shown in Table 1 and did not suggest a superstructure. Therefore we believe the current model is correct.

As in any Al/Si-containing intermetallic compounds, Al and Si are difficult to distinguish by X-ray scattering. The current model gives the lowest $R$ values, best temperature factors, and most reasonable composition compared to the observed EDS analysis. More significantly, however, the bond distances in the chosen model agree well with corresponding distances in the literature. It was found in the title compound that the shortest and/or average bond distances of M−Si are shorter than corresponding M−Al distances, where M can be Sm, Si, or Al. By looking at the bond distance table (Table 4), we can find the following average distances:

$$\text{Sm−Si (3.077 Å)} < \text{Sm−Al (3.314 Å)}$$

$$\text{Si−Si (2.436 Å)} < \text{Si−Al (2.644 Å)} < \text{Al−Al (2.857 Å)}$$

There is no pure Ni−Si distance in the compound, and therefore the comparison between Ni−Si and Ni−Al cannot be made. Considering the disordered Ni/Si site, the average {Ni(1)/Si(1)}−Si distance (2.480 Å) is slightly longer than the Ni−Al distance (2.442 Å); however, the shortest {Ni(1)/Si(1)}−Si distance (2.408 Å) is shorter than the Ni−Al distance.

Because of the inability to resolve Al from Si, there is a possibility that Si(2) and Si(3) are actually aluminum. This, however, is inconsistent with the EDS analyses. Nevertheless, we will investigate this issue further with neutron diffraction experiments.

**Other Physical Methods.** Electron diffraction was performed on a JEOL 100CX transmission electron microscope using an electron beam generated by a $CeB_6$ filament and an accelerating voltage of 120 kV. Samples were prepared by first grinding selected crystals under acetone and then dipping a carbon coated copper grid into the crystal suspension.

Magnetic susceptibilities were measured with a Quantum Design SQUID magnetometer at temperatures between 2 and 300 K.

DC electric conductivity and thermopower measurements were made on single crystals. Conductivity measurements were performed in the usual four-probe technique.[20] Thermopower measurements were made by using a slow ac technique[21] as described elsewhere.[22]

Mass spectrometry was performed on a TRIO-1 GC-MS with $Sm_2Ni(Ni_xSi_{1-x})Al_4Si_6$, which was dissolved in a diluted HCl(aq) solution and the gas produced was collected in a vial over the solution.

**Electronic Band Structure Calculations.** The disordered site of $Sm_2Ni(Ni_xSi_{1-x})Al_4Si_6$ is mainly occupied by silicon atoms ($x = 0.18-0.27$). To understand the origin of this disordered site and probe its influence on the physical properties and stability of the compound, band structure calculations were carried out using the extended Hückel-tight binding method,[23] with the parameters and exponents reported in

(20) Lyding, J. W.; Marcy, H. O.; Marks, T. J.; Kannewurf, C. R. *IEEE Trans. Instrum. Meas.* **1988**, *37*, 76−80.

(21) (a) McCarthy, T. J.; Ngeyi, S.-P.; Liao, J.-H.; DeGroot, D.; Hogan, T.; Kannewurf, C. R.; Kanatzidis, M. G. *Chem. Mater.* **1993**, *5*, 331−340. (b) Chaikin, P. I.; Kawk, J. F. *Rev. Sci. Instrum.* **1975**, *46*, 218−220.

(22) Marcy, H. O.; Marks, T. J.; Kannewurf, C. R. *IEEE Trans. 1nstrum. Meas.* **1990**, *39*, 756−760.

(23) (a) Whangbo, M.-H.; Evain, M.; Hoffmann, R. *EHMACC, Program for Extended Hückel Molecular and Crystal Calculations, North Carolina State University*; 1987. (b) Whangbo, M.-H.; Hoffmann, R. *J. Am. Chem. Soc.* **1978**, *100*, 6093−6098. (c) Hoffmann, R. *J. Chem. Phys.* **1963**, *39*, 1397−1412.

**Table 4. Selected Bond Distances (Å) and Angles (deg) $Sm_2Ni(Ni_xSi_{1-x})Al_4Si_6$ ($x = 0.27$)**

Bond Distances (Å)

| | | | | | |
|---|---|---|---|---|---|
| Sm−Si(1)/Ni(1) | 4x | 3.223(1) | Si(2)−Al | 4x | 2.625(2) |
| Sm−Si(2) | 4x | 3.073(1) | Si(3)−Al | 4x | 2.662(3) |
| Sm−Si(3) | 4x | 3.0297(9) | Si(4)−Si(4) | | 2.407(4) |
| Sm−Si(4) | 4x | 3.128(1) | | 2x | 2.451(3) |
| Sm−Al | 4x | 3.314(1) | Al−Al | | 2.647(3) |
| Ni−Al | 8x | 2.4425(9) | | 2x | 2.856(2) |
| Si(1)/Ni(1)−Si(2) | | 2.408(4) | | 2x | 2.950(2) |
| Si(1)/Ni(1)−Si(4) | | 2.551(2) | | | |

Bond Angles (deg)

| | | | | | |
|---|---|---|---|---|---|
| Si(1)/Ni(1)−Sm−Si(1)/Ni(1) | | 128.5(1) | Sm−Al−Si(2) | 2x | 61.03(5) |
| Si(1)/Ni(1)−Sm−Si(2) | 2x | 173.40(7) | Sm−Al−Si(3) | 2x | 59.75(5) |
| | 2x | 44.89(7) | Ni−Al−Ni | | 114.37(7) |
| Si(1)/Ni(1)−Sm−Si(3) | 4x | 97.14(3) | Ni−Al−Al | 2x | 52.85(3) |
| Si(1)/Ni(1)−Sm−Si(4) | 4x | 47.34(5) | | 2x | 54.22(3) |
| | 4x | 91.62(5) | | 2x | 57.19(3) |
| Si(2)−Sm−Si(2) | | 141.7(1) | | 2x | 125.77(3) |
| Si(2)−Sm−Si(3) | 4x | 84.61(2) | | 2x | 127.15(3) |
| Si(2)−Sm−Si(4) | 4x | 82.82(6) | Ni−Al−Si(2) | 2x | 108.54(4) |
| | 4x | 127.98(5) | Ni−Al−Si(3) | 2x | 111.30(4) |
| Si(3)−Sm−Si(3) | | 146.7(1) | Sm−Si(1)/Ni(1)−Sm | 4x | 79.12(4) |
| Si(3)−Sm−Si(4) | 4x | 72.55(6) | | 2x | 128.5(1) |
| | 4x | 136.70(6) | Sm−Si(1)/Ni(1)−Si(2) | 4x | 64.25(5) |
| Si(4)−Sm−Si(4) | 2x | 46.14(7) | Sm−Si(1)/Ni(1)−Si(4) | 8x | 64.37(3) |
| | 2x | 64.86(7) | | 8x | 138.77(2) |
| | 2x | 83.24(5) | Si(2)−Si(1)/Ni(1)−Si(4) | 4x | 111.58(8) |
| Si(1)/Ni(1)−Sm−Al | 4x | 87.32(5) | Si(4)−Si(1)/Ni(1)−Si(4) | 4x | 82.22(5) |
| | 4x | 136.82(5) | | 2x | 136.8(2) |
| Si(2)−Sm−Al | 4x | 48.36(5) | Sm−Si(2)−Sm | 4x | 83.82(3) |
| | 4x | 98.60(6) | | 2x | 141.7(1) |
| Si(3)−Sm−Al | 4x | 49.37(5) | Sm−Si(2)−Al | 8x | 70.62(3) |
| | 4x | 101.65(6) | | 8x | 136.88(4) |
| Si(4)−Sm−Al | 4x | 100.32(4) | Sm−Si(2)−Si(1)/Ni(1) | 4x | 70.85(5) |
| | 4x | 121.12(4) | Sm−Si(3)−Sm | 4x | 85.30(3) |
| | 4x | 131.05(4) | | 2x | 146.7(1) |
| | 4x | 173.93(4) | Sm−Si(3)−Al | 8x | 70.88(3) |
| Al−Sm−Al | 2x | 51.05(5) | | 8x | 134.47(6) |
| | 2x | 52.88(5) | Al−Si(3)−Al | 4x | 64.89(7) |
| | 2x | 76.57(6) | | 2x | 98.7(1) |
| Al−Ni−Al | 4x | 65.63(7) | Sm−Si(4)−Sm | | 82.03(5) |
| | 4x | 71.55(7) | Sm−Si(4)−Si(1)/Ni(1) | 2x | 68.29(6) |
| | 4x | 74.31(7) | Sm−Si(4)−Si(4) | 2x | 66.93(4) |
| | 8x | 107.07(3) | | 2x | 122.43(4) |
| | 4x | 114.40(7) | | 2x | 133.92(6) |
| | 4x | 178.43(6) | Si(1)/Ni(1)−Si(4)−Si(4) | | 96.2(1) |
| Sm−Al−Sm | | 76.75(6) | | 2x | 131.11(3) |
| Sm−Al−Ni | 2x | 84.18(3) | Si(4)−Si(4)−Si(4) | | 90.0 |
| | 2x | 160.88(8) | | 2x | 100.82(7) |
| Sm−Al−Al | 2x | 63.57(2) | | | |
| | 2x | 64.48(2) | | | |
| | 2x | 115.53(2) | | | |
| | 2x | 116.43(2) | | | |
| | 2x | 141.67(2) | | | |

Table 5. The nondiagonal $H_{ij}$ matrix elements were calculated by using the modified Wolfsberg−Helmholz formula.[24]

Preliminary calculations showed that the Sm 4f orbitals remain at the energy level of the Sm 4f ionization potential and that these bands are not dispersed. This indicates that these 4f orbitals are not involved in the electronic structure of the compound, in agreement with all previous calculations undertaken so far for the lanthanides.[25] Thus in this study, the calculations were carried out without the 4f orbitals of the Sm atoms.

## Results and Discussion

Molten Al is a good solvent for Si. The phase diagram of Al and Si shows that they form a eutectic system with a eutectic point of 577 °C at 12.2% mol of Si.[26] In addition, Al metal does not react with Si, a very important factor that makes Al metal suitable for the synthesis and crystal growth of silicides. This is supported by the fact that Si crystals are frequently found in the reaction products. With rapid Si diffusion in the melt comes increased reactivity with the other metals, which initiates phase formation. Most elements are to a certain extent soluble in Al and, in this sense, the flux reaction is not, philosophically, different from any conventional solvent. Therefore, based on the temperature and time, both kinetic or thermodynamic phases can form. Here we describe the reaction of Sm, Ni, and Si in molten Al. The resulting well-formed and relatively large crystals of $Sm_2Ni(Ni_xSi_{1-x})Al_4Si_6$, see Figure 1, imply that there probably is considerable solubility in Al, not only of the reactants but of any intermediate as well as products species.

(24) Ammeter, J.; Bürgi, H.-B.; Thibeault, J.; Hoffmann, R. *J. Am. Chem. Soc.* **1978**, *100*, 3686−3692.

(25) Ortiz, J. V.; Hoffmann, R. *Inorg. Chem.* **1985**, *24*, 2095−2104.

(26) Binary Alloy Phase Diagrams, Editor-in-chief, Massalski, T. B., American Society for Metals, Metals Park, OH, 1986.

**Table 5. Exponents and Parameters Used in the Calculations; Contraction Coefficients Used in the Double−$\zeta$ Expansion ($C_1$ and $C_2$)**

| atom | orbital | $H_{\mu\mu}$, eV | $\zeta_1$ | $C_1$ | $\zeta_2$ | $C_2$ | ref |
|---|---|---|---|---|---|---|---|
| Al | 3s | −12.3 | 1.167 | | | | (a) |
| | 3p | −6.5 | 1.167 | | | | |
| Ni | 4s | −10.95 | 2.10 | | | | (b), (c) |
| | 4p | −6.27 | 2.10 | | | | |
| | 3d | −14.20 | 5.75 | 0.5683 | 2.30 | 0.6292 | |
| Si | 3s | −17.30 | 1.383 | | | | (d) |
| | 3p | −9.20 | 1.383 | | | | |
| Sm | 6s | −4.86 | 1.400 | | | | 25 |
| | 6p | −4.86 | 1.400 | | | | |
| | 5d | −6.06 | 2.747 | 0.7184 | 1.267 | 0.4447 | |
| | 4f | −11.28 | 6.907 | 0.7354 | 2.639 | 0.4597 | |

[a] Anderson, A. B.; Hoffmann, R. *J. Chem. Phys.* **1974**, *60*, 4271−4273. [b] Summerville, R. H.; Hoffmann, R. *J. Am. Chem. Soc.* **1976**, *98*, 7240−7254. [c] Lauher, J. W.; Elian, M.; Summerville, R. H.; Hoffmann, R. *J. Am. Chem. Soc.* **1976**, *98*, 3219−3224. [d] Trong Anh, N.; Elian, M.; Hoffmann, R. *J. Am. Chem. Soc.* **1978**, *100*, 110−116.

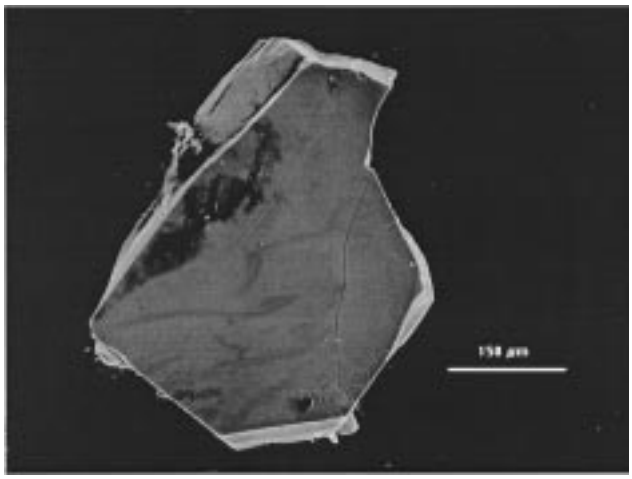


**Figure 1.** Typical scanning electron microscope image of an Al-flux grown crystal (method 2) of $Sm_2Ni(Ni_xSi_{1-x})Al_4Si_6$.

In addition to metals, metal oxides can be used as reactants. The oxide precursor method tends to given low yield of product (2−15%) but often produces crystals with very good morphologies. When metal oxides are used, Al metal serves not only as a flux but also a reducing agent for the oxide. The formation energy of $Al_2O_3$ is much higher than those of any transition metal and rare earth metal oxides and therefore provides a very powerful driving force for this reduction. The metals, formed in-situ from the reduction of the oxide precursors, are in a finely divided, more reactive state than bulk metals. Thus, the reaction can be carried out at relatively low temperature (eq 1).

$$Sm_2O_3 + (1 + x)NiO + ([2(10 + x)]/3)Al + (7 - x)Si \rightarrow Sm_2Ni(Ni_xSi_{1-x})Al_4Si_6 + [(4 + x)/3]Al_2O_3 \quad (1)$$

In fact a large family of compounds with general formula $Ln_xM_yAl_nSi_m$ (Ln = rare earth metal and M = transition metal; $x$ or $y$ can be zero) can be synthesized in this way.[27] The use of oxide precursors is more economical since oxides are usually cheaper than metals, especially for some rare earth metals.

(27) Chen, X. Z.; Sieve, B.; Small, P.; Kanatzidis, M. G., manuscript in preparation.

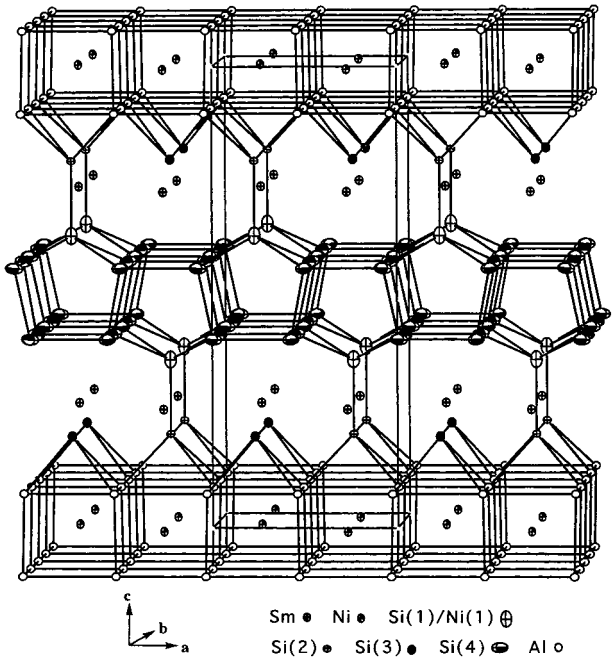


**Figure 2.** Structure of $Sm_2Ni(Ni_xSi_{1-x})Al_4Si_6$. Note the $NiAl_8$ cube layers at the top and bottom of the cell. In the middle there is a layer formed by Si(4) and Si(1)/Ni(1) atoms. The two different layers are connected through Si(1)/Ni(1)−Si(2) bonds. No bonds are drawn around Sm atoms.

To obtain a pure phase of $Sm_2Ni(Ni_xSi_{1-x})Al_4Si_6$, it is necessary to use stoichiometric Sm, Ni, and Si with excess of Al metal. To isolate the compound the excess Al metal can be removed by using a NaOH(aq) solution. The advantage of using oxides, however, becomes even more apparent when ternary and quaternary oxides are used, which bring to the reaction a stoichiometrically fixed combination of elements, which end up in the final aluminum silicide compound.[28]

The black compound $Sm_2Ni(Ni_xSi_{1-x})Al_4Si_6$ ($x = 0.18-0.27$) is stable in air, water, and NaOH(aq) solution (<3 M) but decomposes instantaneously in dilute HCl solution to release a gas which does not ignite upon contact with air. Mass spectrometry showed the gas is hydrogen and did not detect the presence of any silane(s). This is in contrast to $Ln_2Al_3Si_2$ (Ln = Ho, Er, Tm) and $LnAl_2Si_2$ ($Ln$ = La, Sm, Tb, Yb)[29] ($CaAl_2Si_2$-type structure[30]) which, when dissolved in HCl, release silane which ignites upon contact with air on the surface of the solution.

**Structure Description.** The three-dimensional structure of $Sm_2Ni(Ni_xSi_{1-x})Al_4Si_6$ is shown in Figure 2. The compound crystallizes in a new structure type with space group $P4/nmm$ (No. 129). Si(1) and Ni(1) are disordered on the same site with 77% and 23% occupancies, respectively, based on the crystal selected. The Ni-to-Si ratio in this site seems to be relatively fixed around the value of 25%. Even though a large number of synthetic experiments were run with greatly varying Sm/Ni ratios, the final product of $Sm_2Ni(Ni_xSi_{1-x})Al_4Si_6$ gave similar and consistent $x$ values between 0.18 and 0.27 as determined by EDS analyses and by single-

(28) Sieve, B.; Chen, X. Z.; Kanatzidis, M., work in progress.
(29) Chen, X. Z.; Kanatzidis, M. G., manscript in preparation.
(30) Gladyshevskii, K. I.; Kipyakevich, P. I.; Bodak, O. I. *Ukr. Fiz. Zh.* **1967**, *12*, 447−453.

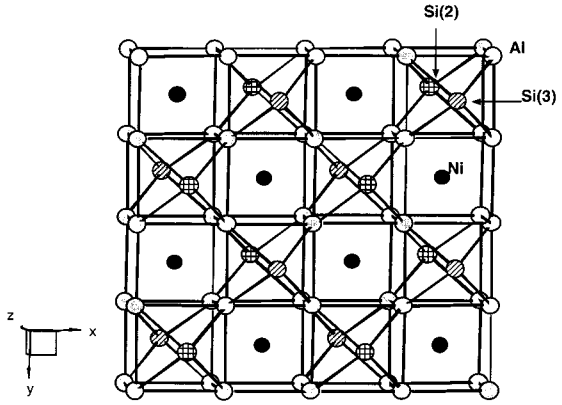


**Figure 3.** $NiAl_8$ cube layer in the *ab* plane. Note that each $NiAl_8$ cube only connects four (not six) other $NiAl_8$ cubes by sharing the four paralleled edges.

**Table 6. Refined Stoichiometries from Four Different Crystals of $Sm_2Ni(Ni_xSi_{1-x})Al_4Si_6$ at Room Temperature (crystals 2, 3, and 4) and −100 °C (crystal 1)**

| | crystal 1 | crystal 2 | crystal 3 | crystal 4 |
|---|---|---|---|---|
| $x$ | 0.19 | 0.18 | 0.23 | 0.27 |
| $a$ (Å) | 5.8214(1) | 5.8161(1) | 5.8191(1) | 5.8060(3) |
| $b$ (Å) | 5.8214(1) | 5.8161(1) | 5.8191(1) | 5.8060(3) |
| $c$ (Å) | 14.8772(3) | 14.8603(3) | 14.9010(1) | 14.845(1) |
| $V$ (Å$^3$) | 504.17(2) | 502.68(2) | 504.59(1) | 500.43(5) |
| $R1$ | 0.0240 | 0.0432 | 0.0247 | 0.0253 |
| $wR2$ | 0.0706 | 0.1010 | 0.0628 | 0.0644 |

crystal structure refinements. The refinements based on four different $Sm_2Ni(Ni_xSi_{1-x})Al_4Si_6$ crystals from three different preparations gave refined $x$ values in a relatively narrow range, see Table 6.

Attempts to prepare the "end-members", i.e., $Sm_2Ni(Ni)Al_4Si_6$ and $Sm_2Ni(Si)Al_4Si_6$, were unsuccessful. Why the observed narrow range of Ni/Si ratios is preferred is an interesting issue which may have to do with the stability of the entire structure (see below).

The structure of $Sm_2Ni(Ni_xSi_{1-x})Al_4Si_6$ contains two different types of alternating layers which are linked along the *c*-axis by Si−Si and Si−Ni bonds. The first layer is five atomic layers thick with a stacking sequence SiAlNiAlSi. The Ni atoms occupy the centers of distorted Al cubes, see Figure 3b. Each of these $NiAl_8$ cubes shares its four parallel edges with other four $NiAl_8$ cubes to make an infinite layer; see Figures 2 and 3. The $NiAl_8$ cubic coordination is known in NiAl, which has a CsCl-type structure,[31] and in $SmNiAl_4Ge_2$.[32] In $Sm_2Ni(Ni_xSi_{1-x})Al_4Si_6$ the cube dimensions are 2.647 × 2.856 × 2.950 Å, while those in NiAl are 2.88 × 2.88 × 2.88 Å and those in $SmNiAl_4Ge_2$ are 2.748 × 2.936 × 2.748 Å. Therefore, there is Al−Al bonding in the structure of $Sm_2Ni(Ni_xSi_{1-x})Al_4Si_6$.

The second type of layer in $Sm_2Ni(Ni_xSi_{1-x})Al_4Si_6$ is formed by Si(1)/Ni(1) and Si(4) atoms (Figures 2 and 4). This Si-based layer is two atomic layers thick and consists of four-member planar rings formed by Si(4) atoms [Si(4)−Si(4) bond 2.450 Å], five-member rings formed by four Si(4) and one Si(1)/Ni(1) atoms, and six-member rings (boatlike) formed by four Si(4) and two Si(1)/Ni(1) atoms [Si(4)−Si(1)/Ni(1) bond 2.564 Å]. The square and hexagonal rings can be seen clearly in Figure 4b while five-member rings are better viewed from Figure 2 and Figure 4a. Si hexagonal nets are known in several silicides. For example, $CaSi_2$ and $\beta$-$USi_2$ both contain hexagonal Si rings. The Si-based layer, shown in Figure 4, is a unique feature of the structure of $Sm_2Ni(Ni_xSi_{1-x})Al_4Si_6$. The different coordination environments for the four different Si atoms in $Sm_2Ni(Ni_xSi_{1-x})Al_4Si_6$ are shown in Figure 5. Selected bond distances and angles are listed in Table 4.

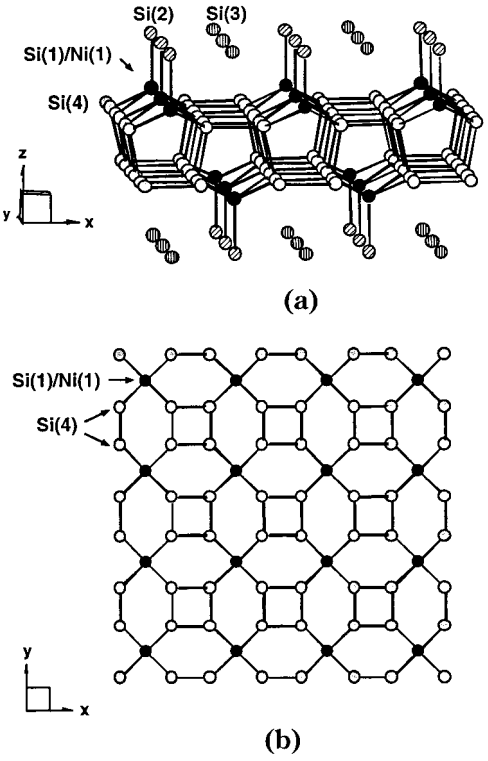


**Figure 4.** (a) The double "Si"-net formed by Si(4) and Si(1)/Ni(1) atoms; (b) half of the net which is obtained by cutting the one in (a) at the middle in the *ab* plane.

If we consider the ideal stoichiometry where $x = 0$, we see that the structure possesses a thick, two-dimensional infinite layer of Si shown in Figure 4a. Therefore, a striking feature of this structure type is the complete segregation of Al and Si atoms in different parts of the cell, in sharp contrast to aluminum silicate compounds where there tends to be maximum dispersion of these elements in the oxide lattice.

There are three different types of Si atoms in this layer, terminal atoms (Si(2)) on both sides of the layer, five-coordinate atoms, and four-coordinate distorted tetrahedral atoms. It is the five-coordinate sites which accommodate in part Ni atoms. From a coordination chemistry point of view, the Si/Ni disorder in this site is surprising (though not unprecedented), given that in most cases in conventional compounds these two elements display very different chemistry. Nevertheless, it is also surprising to see that Si and Ni, in fact, possess very similar Pauling electronegativities (1.9 and 1.91) and size and these characteristics may be, to a certain extend, responsible for their preference of the same crystallographic site.

**Electronic Structure.** The main goal of the band structure calculations is to check if the stoichiometry on the disordered site significantly affects the stability of the compound and to gain some insight into the

(31) Dutchak Ya. I.; Chekh V. G. *Russ. J. Phys. Chem.* translated from *Zh. Fiz. Khim.* **1981**, *55* (9), 1326−1328.
(32) Chen, X. Z.; Kanatzidis, M. G., manscript in preparation.

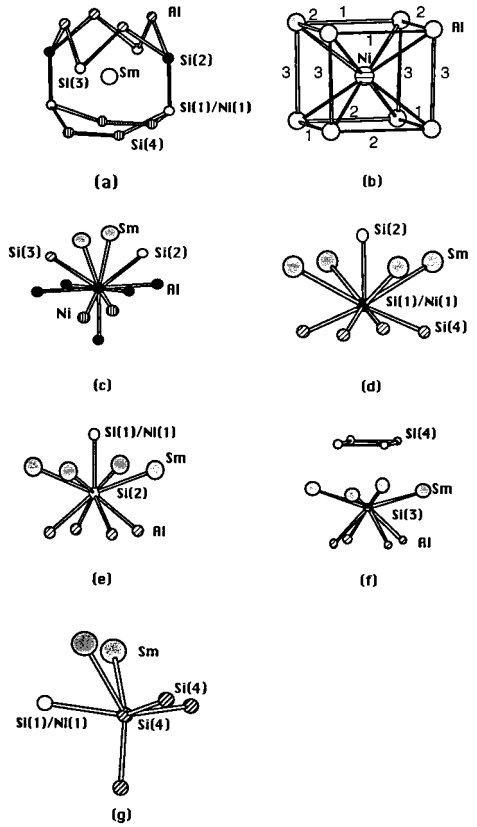


**Figure 5.** Local coordination environments for different atoms.

electrical properties of the material and into the relative valence electron distribution over the different elements.

A mixed site cannot be described by an average atom in the extended Hückel theory (EHT) tight binding method, unlike in a crystal structure refinement. Usually the disordered cases are undertaken by using one of two methods: one considers that the disordered site is fully occupied by the element which possesses the highest occupancy or one creates a hypothetical supercell which allows a description of the compound with only fully occupied sites. We have thus investigated five hypothetical occupancy models, for $Sm_2Ni(Ni_xSi_{1-x})Al_4Si_6$, with $x$ equal to 0, 0.25, 0.5, 0.75, and 1.

In this compound the unit cell contains only two symmetry related disordered sites. The models with $x = 0$, 0.5, and 1 can thus be described in the crystallographically determined unit cell. In contrast, a hypothetical supercell is needed to study the models with $x = 0.25$ and 0.75.[33] Two choices are possible to generate the supercell, (a) double the $a$ axis or (b) double the $c$ axis. The supercell obtained by doubling the $a$ axis gives alternate homoatomic and heteroatomic layers corresponding to the previously disordered atomic site, Wyckoff position *2c* in the space group $P4/nmm$. Doubling the unit cell along the $c$ axis generates only homoatomic layers. We first checked for differences between these supercells. A preliminary tight binding band structure calculation for each supercell was performed for $x = 0.25$. The calculated density of states (DOS)[34] and crystal orbital overlap populations (COOP)[33,35] show no significant difference between the two supercells. Consequently no preferential ordering can be highlighted in this structure, which is in agreement with the fact that no supercell was found by X-ray and electron diffraction. The following discussion will only consider the 2$a$ (doubling) supercell.

To the extent that relative stability can be judged by the position of the Fermi level with respect to peaks and valleys in the total density of states, the band structure calculations, undertaken for the three models with $x = 1$, 0.75, and 0.5, indicate that these compositions are less stable relative to those with $x = 0$ and $x = 0.25$. Surprisingly their corresponding total density of states (DOS) for the models $x = 0$ and $x = 0.25$ are identical, see Figure 6a. In the calculated band structure for the $Sm_2Ni(Ni_xSi_{1-x})Al_4Si_6$ (with $x = 0$ and 0.25 (Figure 7)) 3D network, a set of 10 and 25 undispersed bands (respectively for the models with $x = 0$ and 0.25) are exclusively Ni 3d in character. These bands are laying at the energy of the Ni 3d ionization potential, suggesting that the Ni d orbitals do not play an important role in the electronic structure of this material. The lowest energy bands between −21 and −15.5 eV are very dispersive, because of a strong mix between the Si orbitals and the Al orbitals. In both models, the bands immediately below the Fermi level contain contributions from all the atoms but are dominated by the silicon orbitals. The position of the Fermi level for the model with $x = 0$ ($E_F = -6.7$ eV, 108 electrons) implies a semiconducting behavior and corresponds to a metal for the model with $x = 0.25$ ($E_F = -7.2$ eV, 222 electrons); see Figures 6 and 7. Given the fact that EHT tight binding calculations tend to greatly overestimate band gaps, often by manyfold, and the fact that the calculated gap here is indirect and very narrow, about 0.1 eV, we question the actual presence of any such gap in the material with $x = 0$. The predicted metallic behavior of the model with $x = 0.25$ is in agreement with the electrical conductivity measurements; see below.

It is also worth pointing out that the energy of the Fermi level obtained for the model with $x = 0$ corresponding to 108 electrons (i.e., crystallographic unit cell) is higher than for the model with $x = 0.25$ (i.e., corresponding to 222 electrons, empirical supercell). This difference is due to the addition of 15 low-energy d orbitals for Ni. These d orbitals are filled up and play the role of electron sink, decreasing the energy of the Fermi level. Another interesting point is that the d orbitals of the nickel atoms are fully occupied. The nickel atoms should therefore be nonmagnetic, which is supported by the magnetic measurements; see below.

The magnetic susceptibility measurements of the compound (for all values of $x$ examined) point to $Sm^{3+}$ atoms, not surprisingly since it has the lowest Pauling electronegativity. The Ni on the other hand is one of the most electronegative elements in the structure (along with Si). At least based on electronegativity arguments, Ni is likely to accept electrons either from Sm or from Al,[36] and this is very much in agreement with the results of the band structure calculations,

(33) This requires a triclinic Brillouin zone.

(34) Hoffmann, R. *Angew. Chem., Int. Ed. Engl.* **1987**, *26*, 846−878.

(35) Hughbanks, T.; Hoffmann, R. *J. Am. Chem. Soc.* **1983**, *105*, 1150−1162.

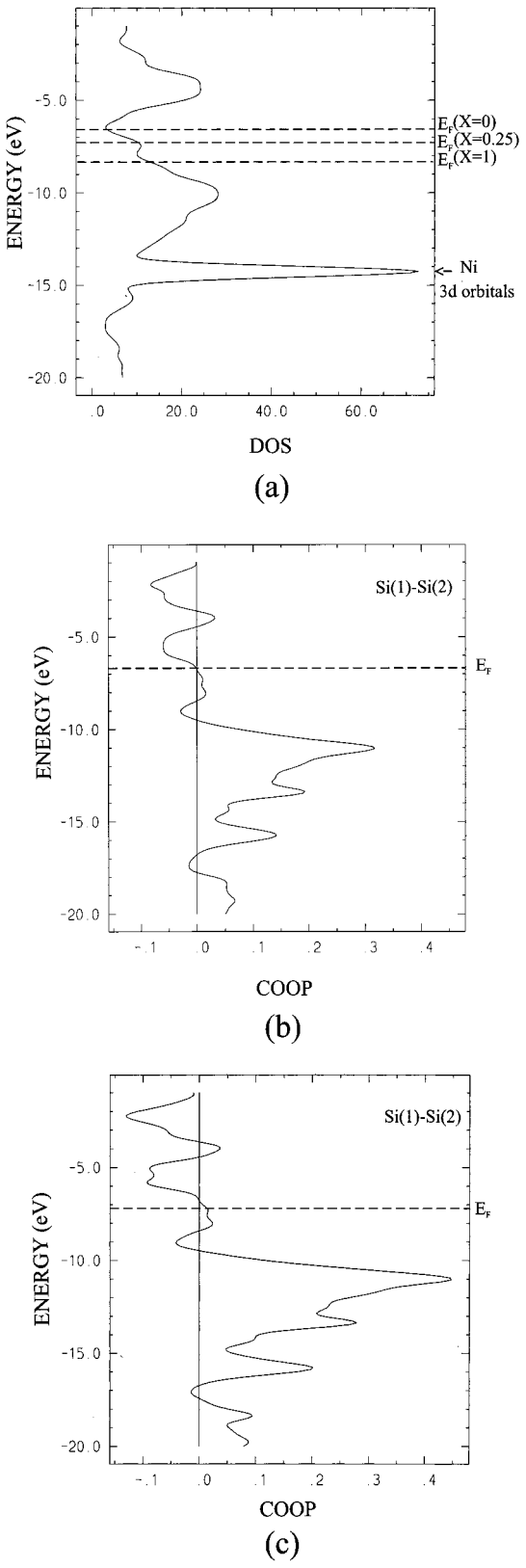


**Figure 6.** (a) Total density of states for $Sm_2Ni(Ni_xSi_{1-x})Al_4Si_6$ compound for $x = 0$, 0.25, or 1 with the corresponding Fermi levels ($E_F = -6.7$, $-7.2$, and $-8.2$ eV, respectively). (b) COOP curve for the Si(2)−Si(1) interaction in $Sm_2Ni(Ni_xSi_{1-x})Al_4Si_6$ for $x = 0$. (c) COOP curve for Si(2)−Si(1) interaction in $Sm_2Ni(Ni_xSi_{1-x})Al_4Si_6$ for $x = 0.25$.

which show that the Ni d orbitals are completely filled. A reasonable assumption is that Ni in this compound possesses a formal charge of 0 or −1, and thus this

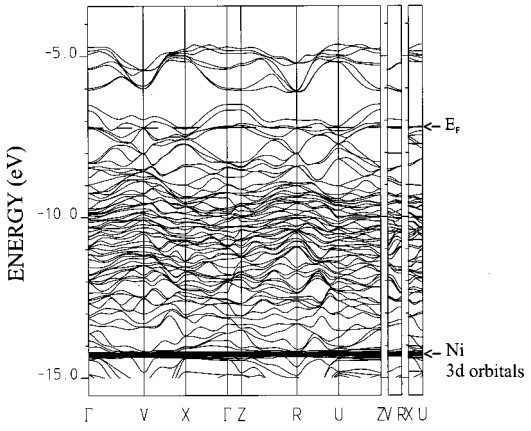


**Figure 7.** Calculated band structure for $Sm_2Ni(Ni_xSi_{1-x})Al_4Si_6$ compound with $x = 0.25$. The Fermi level, dash line, was drawn for the 222 electrons contained in the repeat unit made of 56 atoms. In this calculation, the irreducible part of the triclinic Brillouin zone is limited by the special $k$ points: Γ(0,0,0), X(1/2,0,0), V(1/2,1/2,0),Z(0,0,1/2), U(1/2,0,1/2), and R(1/2,1/2,1/2).

compound is not a Zintl phase. That $Sm_2Ni(Ni_xSi_{1-x})Al_4Si_6$ is not a Zintl phase or a Hume−Rothery phase can also be gleaned from the average valence electron count (VEC) of ∼3.

The electron densities provide the charge distribution in the lattice, and in all models which were studied, the Ni atoms are calculated to be the most reduced (electron densities 12.99 and 12.84 for Ni and 12.02 for Ni(1) for both electron counts). In addition to the Sm atoms, the Al atoms are the most oxidized with electron densities between 2.20 and 2.19. The most reduced silicon atom is Si(3) (bound to Al) with electron densities of 5.02 and 4.97. The Si(4) atoms stay neutral (electron densities 3.99 and 3.92), which is consistent with the distorted tetrahedral coordination. An electron transfer is suggested from Si(1) to Si(2), with electron densities of Si(1) and Si(2) respectively 3.59 and 5.02.

A careful observation of the density of states (DOS) and crystal orbital overlap population (COOP) (Figure 6) shows that, for both models ($x = 0$ and 0.25), the Fermi level lies in an area of nonzero DOS but falls in a deep valley. This energy level falls also in a zone of crossover between bonding and antibonding levels in the Si(2)−Si(1) COOP, which indicates that at $0 < x < 0.25$ optimized bonding is achieved.

Although it seems that the hypothetical stoichiometry, $x = 0$, is slightly more stable than the observed $x = 0.25$, both compounds seem energetically very close.

At higher $x$ values (for example, $x = 1$ in Figure 6a) the Fermi energy level decreases and lies in a region with much higher DOS. This suggests that the system is destabilized at higher $x$ values (i.e., higher Ni content on the disordered site) and is consistent with the fact that, despite many synthetic attempts with high Ni:Sm ratios (>3:1), no value of $x$ greater than 0.3 has been observed. In fact, a different phase emerges when the high Ni:Sm ratios (>3:1) are used.[37] If the $x = 0$ stoichiometry is supposed to be the most thermo-

(36) Of course, we understand that electron−electron interaction and exchange interactions could affect this hypothesis or at least render it more qualitative.

(37) Sieve, B.; Chen, X. Z.; Kanatzidis, M., work in progress.

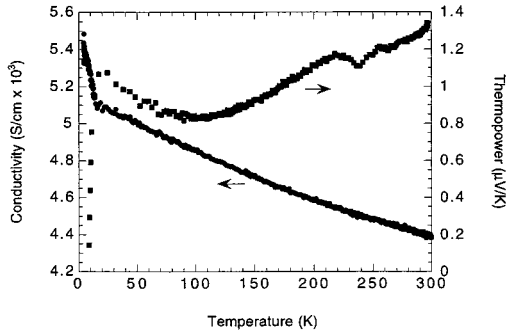


**Figure 8.** Variable-temperature single-crystal electrical conductivity and thermopower data for $Sm_2Ni(Ni_xSi_{1-x})Al_4Si_6$ ($x = 0.18-0.27$)

dynamically stable composition, why have we not been able to achieve it, even when we prepared the compound from Sm/Ni ratios higher than 3:1. For example, a reaction with Sm/Ni as high as 4:1 gave the compound with $x = 0.19$. Perhaps compositions with $0.18 < x < 0.3$ have high kinetic stability and arise because of the similar electronegativities of Ni and Si. A consequence of this could be that once some Ni atoms spill over into the Si(1) site, they become trapped.

**Properties.** The variable-temperature electrical conductivity and thermopower data on several single crystals of $Sm_2Ni(Ni_xSi_{1-x})Al_4Si_6$ are shown in Figure 8. The conductivity typically varies from 4000 to 6000 S/cm and rises with falling temperature. The charge transport properties seem to be insensitive to $x$ and are in agreement with the band structure calculations, which predict metallic behavior at any $x > 0$. The very small positive thermopower at room temperature (<1.4 $\mu$V/K) is also consistent with the metallic behavior of the compound and suggests a p-type conductor.

The temperature-dependent magnetic susceptibility exhibits a broad maximum near 75 K as well as temperature-independent Pauli paramagnetism (TIP) of approximately $1.8 \times 10^{-3}$ emu/mol; see Figure 9. A fit to the high-temperature data, corrected for TIP, gives a $\mu_{eff}$ value of 0.96 $\mu_B$ (see inset to Figure 9A), which is remarkably close to the theoretical value for $Sm^{3+}$ of 0.84. There appears to be no magnetic moment on the nickel atom as has also been observed in many $LnNiT_2$ compounds (Ln = rare earth metal; T = Si, Ge) which were studied by neutron diffraction.[38]

In addition there is a transition to a weak ferromagnetic (WF) state in $Sm_2Ni(Ni_xSi_{1-x})Al_4Si_6$ near 17 K with a field-cooled magnetization which is 40 times as large as the zero-field-cooled magnetization at 2 K. The WF characterization derives from the very broad and very difficult to saturate hysteresis loop shown in Figure 10. The broad maximum in the susceptibility could be due two-dimensional antiferromagnetic coupling between the $Sm^{3+}$ atoms in the *ab* planes, while the three-dimensional WF state is due to ferromagnetic coupling between the Sm layers. It is interesting that the WF transition is somewhat difficult to reproduce from batch to batch and can be easily retarded by small changes in the preparation procedure of the material and possibly by varying the value of $x$. The details of this phenomenon seem to be relatively complex and more work is needed to explore the effect $x$ has on the occurrence of the transition.

(38) Gil, A.; Szytula, A.; Tomkowicz, Z.; Wojciechowski, K. *J. Magn. Magn. Mater.* **1994**, *129*, 271−278 and refs 7 and 8 therein.

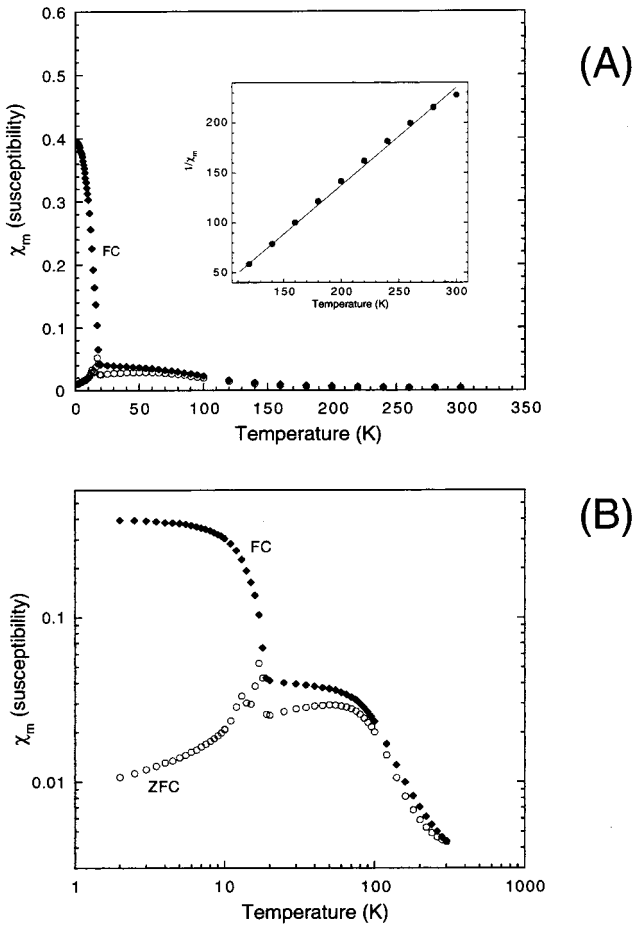


**Figure 9.** (A) Plot of the molar magnetic susceptibility $\chi_m$ (emu/mol) as a function of temperature (K). Inset: Plot of $1/\chi_m$ (mol/emu) vs temperature (K). (B) A log−log plot of the molar magnetic susceptibility $\chi_m$ (emu/mol) versus temperature (K) to enhance both the broad maximum at ~75 and the ferromagnetic transition at 17 K.

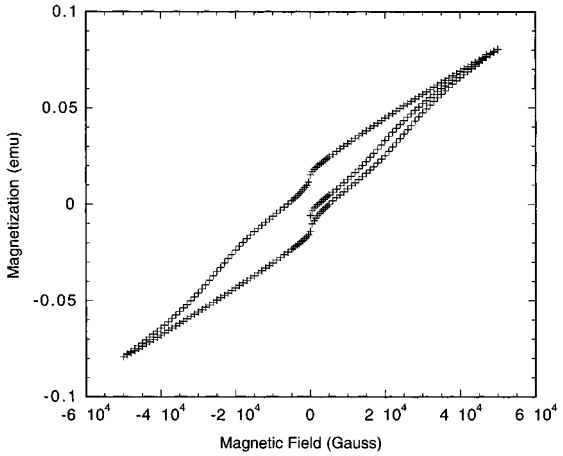


**Figure 10.** Hysteresis loop for $Sm_2Ni(Ni_xSi_{1-x})Al_4Si_6$ at 5 K.

## Conclusion

A new quaternary aluminum silicide $Sm_2Ni(Ni_xSi_{1-x})Al_4Si_6$ with a new structure type and metallic properties has been synthesized from molten aluminum solution.

Recently, we found that the isostructural $Dy_2Ni(Ni_xSi_{1-x})Al_4Si_6$, $Gd_2Ni(Ni_xSi_{1-x})Al_4Si_6$, and $Sm_{2-y}Y_yNi(Ni_xSi_{1-x})Al_4Si_6$ also form from Al flux.[39] This is exciting and underscores the great potential of molten Al as a reaction medium for accessing novel Al-containing multinary silicides. The double Si nets found in the *ab* plane is a unique structural feature which does not seem to obey Zintl's concept. Tight binding band structure calculations for different hypothetical stoichiometries confirm the metallic character of this phase and suggest the compound with $x = 0$ (i.e., pure Si content at the Ni/Si disordered site) to be more stable than the others, but the observed ratio $x = 0.25$ also has good relative stability.

The persistent occurrence of Ni and Si in the same crystallographic site in $Sm_2Ni(Ni_xSi_{1-x})Al_4Si_6$ (under a wide variety of reactant ratios and conditions) is one of the surprises encountered in this work. In the normal day to day discourse of chemistry these two elements appear very different in almost all respects. In $Sm_2Ni(Ni_xSi_{1-x})Al_4Si_6$, however, and we now find in many other RE/M/Al/Si phases prepared with Al flux, the occupation of the same lattice site between Ni and Si seems to be not only common but even necessary for phase stability. One lesson to be learnt here is that, in some respects, Ni and Si may be more similar chemically than we may think, and a clue for this resemblance may be found in the very comparable size and electronegativity of the two elements. How far this relationship can be taken will have to be explored in future investigations of these systems.

(39) The complete details of the synthesis and properties of these materials will be reported later.

**Acknowledgment.** We thank Dr. Mahanti for helpful discussions and suggestions on the magnetic data. M.G.K. is an A.P. Sloan Foundation and Camille and Henry Dreyfus Teacher Scholar 1993−1995. This work made use of the SEM facilities of the Center for Electron Optics at Michigan State University and the facilities of the Materials Research Center at Northwestern University (DMR-96-32472).

**Supporting Information Available:** Tables of fractional atomic coordinates, anisotropic thermal parameters, and bond distances and angles for $Sm_2Ni(Ni_xSi_{1-x})Al_4Si_6$ ($x = 0.19$) (29 pages). See any current masthead page for ordering information and Internet access instructions.

CM980291Z